Downscaling Indonesian Precipitation Using Large-scale Meteorological Fields

Daniel J. Vimont *

Department of Atmospheric and Oceanic Sciences

and Center for Climatic Research

University of Wisconsin - Madison, Madison, WI

David S. Battisti

Atmospheric Sciences Department

University of Washington, Seattle, WA

Rosamond L. Naylor

Program on Food Security and the Environment

Stanford University, Stanford, CA

Corresponding author address: Daniel J. Vimont, 1225 W. Dayton St., Madison, WI 53706.

E-mail: dvimont@wisc.edu

ABSTRACT

This study investigates the skill of linear methods for downscaling provincial-scale precipitation over Indonesia from fields that describe the large-scale circulation and hydrological cycle. The study is motivated by the strong link between large-scale variations in the monsoon and the El Niño – Southern Oscillation (ENSO) phenomenon and regional precipitation, and the subsequent impact of regional precipitation on rice production in Indonesia. Three different downscaling methods are tested across five different combinations of large-scale predictor fields, and two different estimates of regional precipitation for Indonesia.

Downscaling techniques are most skillful over the southern islands (Java and Bali) during the monsoon onset or transition season (Sep.-Dec.). The methods are moderately skillful in the southern islands during the dry season (May-Aug.), and exhibit poor skill during the wet season (Jan.-Apr.). In northern Sumatra downscaling methods are most skillful during Jan.-Apr. with little skill at other times of the year. There is little difference between the three different linear methods used to downscale precipitation over Indonesia. Additional analysis indicates that downscaling methods that are trained on the annual cycle of precipitation produce less-biased estimates of teh annual cycle of regional precipitation than raw model output, and also show some skill at reconstructing interannual variations in regional precipitation. Most of the downscaling methods' skill is attributed to year-to-year ENSO variations and to the long-term trend in precipitation and large-scale fields.

While the goal of the present study is to investigate the skill of downscaling methods

specifically for Indonesia, results are expected to be more generally applicable. In particular, the downscaling models derived from observations have been effectively used to debias the annual cycle of regional precipitation from global climate models. It is expected that the methods will be generally applicable in other regions where regional precipitation is strongly affected by the large-scale circulation.

1. Introduction

Indonesia's geographical location (situated at equatorial latitudes between the Southeast Asian and Australian land masses, and at longitudes between the Pacific and Indian oceans; Fig. 1) places it in a position to be strongly influenced by the annual march of the Southeast Asian / Austral monsoon system, and by year-to-year fluctuations in the El Niño / Southern Oscillation (ENSO) phenomenon. The climatology of precipitation over Indonesia has been described in detail during the colonial period (Braak, 1929; this extensive work also documents the weather and climate phenomena of the region); with a focus on agricultural production – especially wet season rice (Schmidt and Ferguson 1951; Oldeman 1975; Oldeman *et al.* 1979); and more recently using objective criteria based on the amplitudes of the annual and semi-annual cycle in precipitation (Hamada et al. 2002; Aldrian and Susanto 2003; see also McBride 1998, and Chang et al. 2004, for reviews). In general, the latter classification schemes identify regions that are wet all year round (Northern Sumatra, equatorial Kalimantan and Sulawesi, Papua); and regions that are strongly affected by the Austral monsoon, with rainfall maxima during October-February (central and eastern Java, and the eastern islands in Indonesia's archipelago) (McBride 1998). These classifications follow closely the meridional variations of the monsoon system (Tanaka 1994).

During some years the annual march of the monsoon is altered by large-scale conditions associated with concurrent ENSO events (Haylock and McBride 2003; Aldrian and Sustanto 2003; Hendon 2003; McBride *et al.* 2003; Naylor *et al.* 2007). ENSO is

most strongly related to Indonesian precipitation (particularly over the southern islands) during the dry (June-August) and transition (September-November) seasons, and is largely unrelated to precipitation variations during the height of the wet season (December-February) (McBride and Nicholls 1983; Haylock and McBride 2003; Hendon 2003). During ENSO warm events the strength of the ascending branch of the Walker Circulation over the Maritime Continent is reduced, resulting in decreased precipitation and lower level convergence over the region. These large-scale influences are augmented by local air-sea interaction during the dry season, when increased easterly trade winds generate anomalously cool sea surface temperature (SST) in the region through increased latent heat flux. The cooled SST increases anomalous subsidence in the region through large-scale feedbacks and local hydrostatic arguments (Hackert and Hastenrath 1986; Hendon 2003). During the wet season, the reverse occurs: anomalous easterlies counteract the climatological westerlies over the region, increasing SST through reduced latent heat flux and hence counteracting the effects of large-scale subsidence over the region. Alternatively, it has been argued that once the wet season commences precipitation variations are dominated by synoptic and mesoscale variations that are less sensitive to the large-scale circulation (Haylock and McBride 2003).

Despite the strong relationship between the large scale circulation and monsoonal precipitation, it is important to note that precipitation over Indonesia is heavily influenced by sub-seasonal variability and by small scale variations. In particular, Qian (2008) shows that the regional geography of Indonesia leads to small scale land-sea breezes and mesoscale processes that influence the diurnal cycle and mean intensity

of convection over the region. Houze *et al.* (1981) also points out the importance of diurnal variations, and documents large sub-seasonal variations in rainfall over Borneo during the International Winter Monsoon Experiment that are related to synoptic scale wave activity over the region. Climate models that are capable of simulating present and future large-scale climate variations are typically run at a resolution that is far too coarse to resolve the intricate topography and these small-scale variations that are known to influence monsoonal precipitation over Indonesia. These models also tend to have large biases in their simulation of the hydrological cycle over Indonesia (Neale and Slingo 2003; Naylor *et al.* 2007). In the present study we test the ability of linear methods in both downscaling and debiasing precipitation estimates over Indonesia, given the large-scale circulation.

A motivation for the present work is the strong link between year-to-year variations in Indonesian precipitation and rice production. Rice plantings follow the marked seasonality in rainfall, even in irrigated areas since most irrigation is categorized as "run of the river" (Naylor et al., 2001). In a typical year, most rice is planted early in the "wet season" (October-December), when there is sufficient moisture to prepare the land for cultivation and to facilitate the early rooting of the transplanted seedlings. The main planting period occurs before the peak of the monsoon, because excessive water at the vegetative growth stage hampers rooting and decreases tiller production (De Datta, 1981). During the 90-120 day grow-out period from transplanting to harvest, current rice varieties require 600-1200 mm of water depending on the agroecosystem and the timing of rainfall or irrigation (De Datta, 1981). Whether or not the region is irrigated

is important for gauging the critical amount of precipitation needed throughout the season. A smaller "dry season" planting (April-June) takes place in many, but not all, rice-growing regions of Indonesia following the monsoon. Both the timing and amount of precipitation are thus critical for rice production systems.

Earlier work by Naylor, Falcon and colleagues (2001, 2004) shows that ENSO has been the primary determinant of year-to-year variation in Indonesian rice output over the past three decades, accounting for almost two-thirds of the total variation. During El Niño events, Indonesia's production of rice – the country's primary food staple – is affected in two important ways: delayed rainfall causes the rice crop to be planted later in the monsoon season, thus extending the hungry season (*paceklik*, the season of scarcity) before the main rice harvest; and delayed planting of the main wet season crop may not be compensated by increased planting later in the crop year, leaving Indonesia with reduced rice area and a larger than normal annual rice deficit (Naylor *et al.* 2001).

The present study is motivated by the relationships between interannual climate variations, year-to-year fluctuations in regional precipitation, and rice production in Indonesia. The strong relationship between the large-scale circulation and precipitation over Indonesia leads to the hypothesis that empirical downscaling techniques may be suitable for identifying precipitation variations on a regional scale over Indonesia. In the present study, we test this hypothesis using linear methods to relate features in the large-scale circulation to regional precipitation. We also test the potential upper limit of predictability of regional rainfall in Indonesia from large-scale climate variations. Although the study focuses on a specific region (Indonesia), we expect the techniques

to be generally applicable to other tropical regions where precipitation variations have a signature in the large-scale circulation. We note that these models have also been used in a broader context of identifying whether natural climate variability (including ENSO) will exert a greater impact on Indonesian rice agriculture and food security in 2050 with changes in the mean climate (Naylor *et al.* 2007).

The methodology herein is certainly not the only means of downscaling precipitation over Indonesia. Numerous other methods for downscaling precipitation have been developed by other research efforts; reviews can be found in Christensen *et al.* (2007) and Wilby *et al.* (2004). Other methods include regression approaches (under which our methodologies fall), weather generators (e.g. Markov models), weather classification techniques, and analogue methods. Other researchers have found that some techniques produce enhanced skill when downscaling is applied to daily data, and then aggregated to a monthly time scale (Buishand *et al.* 2004), though the application to daily data does not guarantee a better estimate of monthly variationsi (Widmann *et al.* 2003). The techniques used in the present study have also been employed by Widmann *et al.* (2003) over the Pacific Northwest region of North America, and have shown reasonable skill in estimating daily or monthly 50km×50km resolution precipitation estimates from 1000mb geopotential height, 850mb temperature or humidity, or combinations thereof.

This paper is organized as follows. The data and methodology used in this study are described in Section 2, as well as in Appendices A and B. Results from the various downscaling methods, as well as the skill of those methods, are presented in Section 3. A discussion of results and attribution of skill is presented in Section 4, and a summary

of results are presented in Section 5.

2. Data and Methodology

The focus of the present study is to reconstruct provincial-scale precipitation over Indonesia using large-scale meteorological fields. We investigate downscaling methods using two different estimates of provincial-scale precipitation (described in Section 2a and Appendix A), five different combinations of large-scale meteorological variables (described in Section 2b and Appendix B), and three different statistical techniques (described in Section 2c and Appendix B).

a. Precipitation Data

In this study, precipitation data sets are constructed over Indonesia at a provincial scale that is appropriate for investigating relationships with agricultural production. The spatial scale for precipitation is defined using political and agricultural boundaries that correspond to the same boundaries over which agricultural data are available. Some provinces have been combined to eliminate particularly small delineations between regions (Table 1). In particular, we aggregate precipitation over 24 different political regions, listed in Table 1, and shown in Fig. 1a. Data coverage over these 24 regions is far from uniform, with a large number of stations over Java, the most populated island in Indonesia (Fig. 1b). Data are also averaged over three crop seasons roughly

corresponding to the peak of the Austral monsoon (Jan-Apr; JFMA), the dry season (May-Aug; MJJA), and monsoon "transition" (Austral monsoon onset) season (Sep-Dec; SOND). These seasons are chosen due to their relationships with rice planting on Java as well as the seasonality of the monsoon over Indonesia (Tanaka 1994; Naylor *et al.* 2007).

Two different regional precipitation data sets are constructed and used in this analysis. The first is based on the spatially interpolated, gridded data set from the University of Delaware (Version 1.01 of the 1900-2006 Terrestrial Precipitation product; Matsuura and Willmott (2007); hereafter referred to as UDel). Over Indonesia, that data set is primarily based on station observations from the Global Historical Climate Network, version 2 (GHCN; NCDC 2007a), station observations from the Global Surface Summary of the Day (GSOD; NCDC 2007b), and a background climatology from Legates and Willmott (1990). A provincial scale data set is constructed by simple averaging of the 0.5° by 0.5° UDel data from all grid boxes centered in a given geographical province (Fig. 1b). We also tried aggregating precipitation by averaging the standardized anomalies (the same methodology as the aggregated station data; Hackert and Hastenrath (1986) and Appendix A) and found no difference in results.

Although the interpolation procedure for the UDel data produces a data set with fine-scale resolution (0.5° by 0.5°) the *effective* resolution is ultimately determined by the original station density and interpolation algorithm. Note, for example, the dense station network over Java (9-11) compared to Sulawesi (19-22) in Fig. 1b. In order to interpolate to the original 0.5° by 0.5° grid resolution of the UDel data set, grid

boxes in data-sparse regions must be interpolated from stations that are potentially far from the actual grid box, perhaps even across islands (one-point correlation maps for Java and for Papua, not shown, suggest this may be a problem). This may artificially affect the skill of the downscaling technique, as data for a particular region is actually representative of a much larger area (and hence more closely tied to the large-scale flow used as a predictor). The UDel data set also uses data from stations that may have intermittent reporting over the time period 1950-1999 (Fig. 2), which may lead to spurious discontinuities in the estimated precipitation (Fig. 3).

To provide an additional estimate of regional-scale precipitation in Indonesia, a second, station-based regional precipitation data set is constructed. Station data for the second regional precipitation data set is based on available station data from the GHCN and GSOD data, and the NOAA/NCEP Climate Prediction Center reported precipitation [obtained under the name "NOAA NCEP CPC EVE" from the LDEO INGRID; IRI / LDEO (2007); Ropelewski *et al.* (1985)]. Stations from the three inventories were combined (see Appendix A for details) resulting in 71 stations with >30yr of data (not necessarily continuous) over Indonesia (open circles in Fig. 1). Station data in each province were combined to produce an estimate of precipitation that is representative of precipitation within the province, and that accounts for discontinuities in reported precipitation (Appendix A). This resulted in a Station-based regional precipitation product with data for 21 of the 24 provinces considered in this study (Table 1).

A comparison between various regional precipitation estimates over the island of

Java is shown in Fig. 3, including the UDel-based estimate, the Station-based estimate, a satellite-based estimate from the NOAA Climate Prediction Center (IRI / LDEO 2007), and from the NCEP reanalysis (Kalnay and coauthors 1996). Of these, only the satellite-based product is constructed from a homogeneous record. This comparison also illustrates some of the challenges in defining a "true" precipitation estimate for Indonesia. In particular, there are notable discrepancies between the UDel precipitation estimate and the Station precipitation estimate for various periods, especially from 1994-1998. During this period, the Station-based precipitation estimate shows better agreement with the satellite-derived precipitation product from the CPC (IRI / LDEO 2007). During the 1990 wet season, though, the UDel and satellite-based product are in agreement, while the Station estimate is much lower. In general, the UDel estimate is slightly rainier than the Station-based estimate (about 0.7 mm day^{-1}) and has a more pronounced seasonal cycle with up to 25% more rain during the wet season. Additional comparison between the UDel and Station-based precipitation estimates is listed in Table 1.

Although there are no clear winners in estimated precipitation products, there is a clear loser over Indonesia. The estimate of precipitation from the NCEP Reanalysis (Kalnay et al. 1996) shows large discontinuities in the early 1960's, late 1970's, and early 1990's (perhaps corresponding to the expansion of the radiosonde network, and varying satellite coverage). The Reanalysis demonstrates the large biases that can be introduced by a model-based precipitation parameterization (presumably due to changes in data coverage and biases in model parameterizations). We do note, however, that

inspection of the precipitation variability in the Reanalysis estimate does show some similar variability as the observational products suggesting that despite its problems the Reanalysis precipitation may be useful in some analyses.

b. Large-scale Data

Data from the National Center for Atmospheric Research / National Center for Environmental Prediction (NCEP / NCAR) Reanalysis project (Kalnay et al. 1996; hereafter referred to as the reanalysis) is used to describe the large-scale circulation. We use three different variables or combinations of those variables as predictors for provincial precipitation: sea level pressure (SLP), 850mb specific humidity (SHUM), and 250mb and 850mb zonal wind (UWND). SLP is used due to the strong relationship between precipitation and SLP over Indonesia and concurrent ENSO events (Ropelewski and Halpert 1987); SHUM is used to represent the large-scale hydrological cycle (including possible trends); and UWND is used to characterize the monsoon shear line, which is strongly related to monsoon onset (Hendon and Liebmann 1990; Tanaka 1994). Five different predictor sets are used, and described in Table 2. When combinations of predictors are used (e.g. SLP and SHUM), each field is scaled to have equal variance. The predictor data are defined over the region 20S - 20N, 90E - 180 and are interpolated from a 2.5° by 2.5° grid to a 5° by 5° grid (by spatial averaging). We interpolate so that fine-scale features (e.g. the monsoon shear line in UWND) do not unreasonably affect estimates of downscaled precipitation when large-scale GCM fields are projected

onto the predictor structures.

We also tried using the model-based large-scale precipitation as a predictor for regional precipitation, but the large biases in the modeled precipitation field (e.g. Fig. 3) led to large errors in the downscaled precipitation. As a result, we present results from five combinations of the large-scale predictor fields: *(1)* SLP, *(2)* SHUM, *(3)* SLP+SHUM, *(4)* UWND, and *(5)* UWND+SHUM. These variables, and combinations of these variables, do exhibit some small non-stationary behavior over the time period 1950-1999, especially around the introduction of the radiosonde network in the early record, and in the transition to the satellite era in the late 1970's. We do not attempt to adjust for these biases, except as described in the "annual cycle" method of downscaling below.

c. Methods

We test three different methods for estimating the relationship between large-scale predictor fields and provincial precipitation: Empirical Orthogonal Function / Principal Component (EOF/PC) analysis used with linear regression, Maximum Covariance Analysis (MCA), and Canonical Correlation Analysis (CCA). These three linear methods involve identifying spatial patterns in a predictor field (the large scale field) that relate to spatial patterns in a predictand (regional precipitation). These methods are described in more detail in Bretherton *et al.* (1992), and have been used to downscale precipitation over the Pacific Northwest (Widmann *et al.* 2003). We briefly describe

each method in Appendix B. Each method produces a set of large-scale predictor fields and a corresponding set of maps of regional precipitation. We refer to each methodology / predictor field combination (three different methodologies, five different predictor fields) as an "empirical downscaling model" (EDM) that can be used to translate a new (independent) map of the large-scale circulation into an estimate of regional precipitation. In the present study we only apply the EDM to independent data through our cross-validation methodology (described below). However, each EDM can be applied to general circulation model output to obtain an estimate of regional precipitation from the model's large-scale fields. This will be discussed briefly in Sec. 4.

Regional precipitation for each crop season is predicted using cross-validation. The cross-validation is performed as follows. First, one decade (say, 1950-1959) is removed from a particular crop season, and the remaining 40 seasons are used to train the statistical parameters for the EDM. The resulting EDM is then used to predict the decade that had been removed. The process is repeated for the remaining four decades of data, and then again for the remaining two crop seasons. We also constructed EDMs using all seasons together (results not shown) and found poor performance, which is consistent with findings that relationships between the large-scale flow and hydrology are seasonally dependent (McBride *et al.* 2003). Statistically significant correlations or regressions are inferred when the correlation coefficient exceeds the 95% level using a two-tailed t-test.

Finally, to address possible biases that may be introduced by non-stationarity in the large-scale fields, we also train a set of EDMs on the 12mo annual cycle (with the

grand mean removed) of large-scale fields and regional precipitation (e.g. the covariance matrix used in MCA is defined only over the 12mo seasonal cycle). The 50yr of *actual*, monthly data (retaining the annual cycle, but removing the grand mean) is then fed into the EDM as a predictor, and the predicted precipitation is averaged over each crop season. We then evaluate how interannual variations of predicted precipitation relate to interannual variations in actual precipitation (the annual cycle is removed prior to evaluating the skill of the annual cycle EDMs). No cross-validation is necessary here as the annual cycle that is used to train the downscaling technique is removed prior to evaluating the skill of the annual cycle EDMs in simulating interannual variability. These EDMs – trained only on the annual cycle – may show skill in predicting interannual variations in precipitation if the interannual variations are related to changes in timing of the seasonal cycle (e.g. timing of the monsoon).

3. Results

a. Aggregated results

We begin by discussing results aggregated over all of Indonesia. The average correlation (over all provinces) between the actual precipitation and the predicted (cross-validated) precipitation for the UDel precipitation estimate is shown in Fig. 4. Results are shown as a function of crop season, and as a function of the number of modes retained (see Fig. 4 caption). Fig. 4 demonstrates some common characteristics of the es-

timated precipitation. In general, the correlation increases from JFMA through SOND, with the highest average correlation occurring during SOND (the monsoon transition season). This is consistent with Haylock and McBride (2003), who find that precipitation is more coherent across stations during the dry season (JJA in their analysis) and transition season (SON in their analysis). Despite the better skill during the transition season the average correlation is not high: in the best case, average correlations are near $r = 0.6$. These features are generally true for all three downscaling methods, and for both UDel (Fig. 4) and Station (Fig. 5) precipitation estimates.

In general all three downscaling techniques have similar performance when at least two modes are used, indicating that the different large-scale predictor patterns share similar information. This is also shown in Table 3, which depicts the projection of the leading (unit length) spatial large-scale predictor pattern from each method onto the leading and second predictor patterns from each method, as a function of season. Table 3 uses patterns derived from the entire 50yr data set (no cross-validation is used in Table 3). For brevity, we show only the results from predictor set 4 (UWND). For JFMA and SOND the projections indicate that the spatial structure of the leading mode from any one method is very similar to the leading mode from any other method. The same is true for MCA and CCA during MJJA. In contrast, for the UWND predictor set the leading mode from MCA and CCA has a larger projection onto EOF2 than EOF1 for MJJA (further inspection shows that EOF1 is dominated by the trend, while EOF2 is dominated by ENSO). Inspection of Fig. 4 and 5 shows that for three of the predictor sets (SHUM, UWND, and UWND+SHUM, from further analysis) the leading

EOF mode (right panels) contributes very little to the mean correlation, although the leading MCA and CCA modes do (left and center panels, respectively). Because MCA and CCA are based on the covariance (or correlation) between the large-scale predictors and precipitation the unrelated large-scale variability captured by EOF1 is skipped over in these techniques.

The correlation between actual and estimated precipitation is mildly dependent on the number of modes used to reconstruct precipitation. Note that for CCA, the number of modes is limited by the number of EOFs retained in the EOF prefilter (Appendix B), which is between 2 and 3 for the UDel data, and between 1 and 6 for the Station data. Fig. 4 shows that in general for MCA and CCA, the first mode dominates the correlation skill (with the exception of JFMA, where there is little skill to begin with), with only mild improvements from remaining modes. Similar behavior is seen in the Station data. As discussed above, two modes are necessary for the EOF method during MJJA and SOND.

Fig. 6 highlights differences in results from different large scale predictors by stratifying results from the Station-based analysis as a function of method, predictor variable, and season. In general, all large-scale variables show comparable skill during SOND, with almost no distinction between the large-scale variables for the CCA technique during MJJA or SOND. It is also noteworthy that predictor sets that incorporate UWND (sets 4 and 5) show higher skill during JFMA than other predictor sets, for all techniques. Still, the the mean correlation during JFMA for predictor sets 4 and 5 is not high ($r \approx 0.4$).

b. Regional results

Spatial maps of the cross-validated correlation coefficient between actual and predicted precipitation [using the EOF method with predictor set 4 (UWND) and 2 modes] are shown as a function of crop season for the UDel (in Fig. 7) and Station (Fig. 8) precipitation data. The correlations tend to follow the seasonality of mean precipitation. During JFMA the Austral monsoon is at its peak, and there are no significant correlations in the UDel data over the southern-most islands in Indonesia. This is consistent with earlier findings that precipitation is not coherent during the height of the monsoon (Haylock and McBride 2003). Once the monsoon has begun, precipitation variability is likely dominated by meso- and synoptic scale weather events that have a weaker relationship with the large-scale, time-averaged flow. It is noteworthy that Fig. 8 shows statistically significant positive correlations in the Station data during JFMA over West and East Java, and over Bali, though these correlations are weak ($r \approx 0.4$). In fact, statistically significant correlations during the height of the wet season originate from predictor sets 4 and 5 (both incorporate UWND) in West Java, predictor set 4 (UWND) over East Java, and from predictor sets 1, 3, 4, and 5 (these incorporate SLP and UWND) in Bali. It is not clear whether the results from the UDel or Station-based analysis are closer to "truth". The selective sampling for the Station-based precipitation product may bias the results to the more populated lowland areas, or it may provide a more homogeneous record that is less prone to discontinuities than the UDel data.

During MJJA correlations using the UDel or Station-based data are strongest in equatorial regions (southern Sumatra, Kalimantan, Sulawesi, and Maluku), and weakest in northern (Northern Sumatra) and southern (Java, Bali) regions. In general, equatorial locations tend to have a weaker seasonal cycle in precipitation, and may also be less influenced by seasonality of the large-scale monsoon. During MJJA Northern Sumatra and the southern islands (Java, Bali, Nusa Tenggara) are experiencing relative dry seasons (though dry season is much more pronounced in the southern islands than in Northern Sumatra). Reconstructions using other large-scale variables show similar features.

The largest mean correlations between predicted and actual rainfall during SOND occur over southern Indonesia (Java, Bali, Nusa Tenggara). At this time, correlation coefficients using the Station-based precipitation are large ($r = 0.7$). Correlation coefficients with the UDel data are not as large, as discussed above. In both cases, though, the large correlations suggest that there is a strong connection between the large-scale circulation and precipitation over southern Indonesia during the monsoon transition season. Mean monsoon onset dates range from late-October / early-November in Western Java to mid- to late-December in Bali and Nusa Tenggara (McBride 1998; Tanaka 1994; Hamada *et al.* 2002; Naylor *et al.* 2007). These regions also experience a large annual cycle in rainfall. Thus, rainfall variations during SOND are representative of variations in the timing of monsoon onset (Haylock and McBride 2003; Naylor *et al.* 2007). The large-scale circulation features that accompany monsoon onset are well suited for predicting these variations in the timing of the monsoon onset.

The islands of Java and Bali account for about 55% of the country's total rice production and are thus watched most carefully from a food policy perspective. Agricultural data series for these regions are also longer and more complete than for other provinces in Indonesia, and rainfall-rice relationships on Java and Bali have been well established (Naylor *et al.* 2001). Thus, it is worth further examining the EDMs' skill over these islands. The mean correlation coefficients between predicted and actual precipitation over Java and Bali (provinces 9-12 in Fig. 1 and Table 1) are shown in Fig. 9 (UDel precipitation) and Fig. 10 (station precipitation). In general, the EDMs show similar characteristics over Java and Bali as they do over all of Indonesia (compare with Fig. 4 and 5). Still, notable differences exist. In particular, the UDel based precipitation product exhibits almost no skill in estimating precipitation during JFMA (the peak of the Austral monsoon) for any method (for the Station based precipitation the average correlation coefficient over Java and Bali during JFMA is comparable to the average correlation over all of Indonesia). Also, the average correlation over Java and Bali using the UDel based precipitation during SOND (the transition season) is comparable to the average correlation over all of Indonesia, while the average correlation over Java and Bali in the Station based precipitation estimation is much higher than the average over all of Indonesia. Results over Java and Bali suggest that the large-scale flow is capable of predicting regional-scale precipitation variations associated with the timing of the monsoon onset. This has special relevance to rice production, as timing of rice planting is tied to the timing of the monsoon onset (Naylor *et al.* 2001).

c. Downscaling Using the Seasonal Cycle

The downscaling methodologies described above use EDMs that are developed around anomalies from a particular season. As such, these EDMs are unable to downscale the climatological annual cycle of precipitation, and are subject to inhomogeneities in the data from which they are constructed. Motivated by the seasonality in the mechanisms responsible for the variability in precipitation, and to test the impact of data inhomogeneity in EDM construction, we construct a series of EDMs that are trained on the 12mo annual cycle of precipitation and large-scale fields (i.e. covariance matrices and regression coefficients are estimated across the 12mo seasonal cycle with the grand mean removed). After the annual cycle is reconstructed at a regional scale, the grand mean for each region is added back to the downscaled precipitation. For brevity, we restrict the presentation of results to the EOF methodology using 3 modes.

Fig. 11 shows the annual cycle of actual and estimated precipitation averaged over Java and Bali. The actual and estimated precipitation are taken from the UDel based precipitation analysis. Also shown is the raw estimate of the annual cycle of precipitation for Java and Bali taken from the NCEP reanalysis (estimated at the nearest 2.5° by 2.5° grid point). The latter is shown as an example of the biases in model-based precipitation. Fig. 11 suggests that the downscaling methodology may provide a means for debiasing precipitation estimates from large-scale models (because the large scale predictor fields we use in the EDMs are also from the NCEP reanalaysis). Indeed, Naylor *et al.* (2007) show this is the case. Not surprisingly, percent errors (calculated

as the difference between predicted and observed precipitation, divided by observed precipitation for a given month) are largest in magnitude during the dry season (when precipitation rates are low), and are smallest during the wet season. Given the importance of the timing of monsoon onset, it is reassuring to see that the EDM estimates of the annual cycle are quite close to reality during the transition season (Oct.-Dec.). Results for the Station based precipitation data (not shown) are similar to those for the UDel precipitation data. Inspection of other regions (not shown) indicates that the debiasing effect is slightly less effective in regions with a strong semi-annual cycle (e.g. Aceh and West Sumatra), but in all regions the downscaled annual cycle is in much better agreement with the original UDel estimate than is the NCEP reanalysis estimate. Naylor *et al.* (2007) have extended the use of the annual-cycle based EDMs to show that they are an effective means of downscaling and debiasing climate projections from the suite of models that contributed to the World Climate Research Programme's Coupled Model Intercomparison Project phase 3 (CMIP3) multi-model dataset.

Precipitation variability over Indonesia is strongly related to the timing of the monsoon – a feature that should be captured in the annual cycle. Thus, we investigate the skill with which the annual cycle based EDMs are able to reproduce the *seasonal variations* of precipitation over Indonesia. In the case of the EOF methodology, we obtain the EOFs and PCs of the annual cycle of large-scale fields, and compute regression coefficients of the annual cycle of precipitation onto those PCs. Next, the seasonal anomalies are projected onto the annual cycle EOFs to produce a set of seasonal predictor expansion coefficients, which are then multiplied by their associated regional map of

regression coefficients to produce an estimate of seasonal variations in regional precipitation. The mean correlation between the actual and estimated precipitation for the EDM constructed using the annual cycle of the Station-based precipitation is shown in Fig. 12. For the most part, the EDMs perform much more poorly than their counterparts based on seasonal anomalies, with significant skill coming only from predictor sets 1 and 3 (both involve SLP) and only during MJJA and SOND (dry and transition seasons). Estimates that use UWND as a predictor (sets 4 and 5) show quite poor skill for variability, though these same EDMs perform quite well when estimating the annual cycle. The skill in variable sets 1 and 3 in Fig. 12 suggests that during the dry and transition seasons, year-to-year variations in precipitation and SLP arise through variations in the timing or amplitude of the seasonal cycle.

The spatial distribution of annual cycle based EDM skill is shown in Fig. 13, which can be directly compared to Fig. 8. In general the correlations are weaker using the annual cycle based EDMs, especially during JFMA (monsoon season) when there is almost no skill. However, there is still considerable skill over the equatorial regions and southern islands during MJJA and SOND, with correlations of $r = 0.65$ over Java. Again, the timing and regional dependence shown in Fig. 13 suggests that the physical processes that govern year-to-year precipitation variations produce variations in the timing or amplitude of the seasonal cycle.

4. Attribution and Discussion

In this section, we discuss the results presented above, as well as possible applications of the EDMs to output from global climate models.

Why the EDMs perform well over Indonesia: the annual cycle. The annual cycle based EDMs are an effectve means of debiasing the modelled annual cycle of precipitation over Indonesia because the annual cycle of precipitation is strongly related to large-scale circulation and humidity. These latter fields are generally better represented in models than regional-scale, or even large-scale precipitation. For regions where precipitation variations are tightly connected to the annual cycle, the annual cycle based EDMs are also capable of characterizing the interannual variability in precipitation, suggesting that these interannual variations are related to changes in the timing and amplitude of the seasonal cycle. Results from the annual cycle based EDMs also confirm that these methods may be useful for debiasing model-based estimates of precipitation over Indonesia, or wherever there is a strong relationship between the annual cycle of precipitation and the large-scale circulation.

Why the EDMs perform well over Indonesia: the interannual variability. Fig. 6 shows that the highest correlations between predicted and actual precipitation in the Station based precipitation analysis occurs for predictor sets 3, 4, and 5 (SLP+SHUM, UWND, and UWND+SHUM). Furthermore, Fig. 5 shows that most of that predictability is due to the leading mode from any analysis. Thus, it is worth investigating the large-scale conditions associated with that leading statistical mode of variability. Fig. 14

shows the correlation map of SST, SLP, 850 mb zonal wind, and regional precipitation with the leading principal component of the UWND field (predictor set 4) for SOND. The spatial structure of the correlation maps bear a strong resemblance to the structure of an El Niño event (a positive ENSO event) during SOND. The SST pattern has been discussed in relation to Indonesian precipitation (Haylock and McBride 2003; Aldrian and Sustanto 2003; Hendon 2003; McBride *et al.* 2003). The SLP pattern bears the signature of the Southern Oscillation (Walker and Bliss 1932) with low pressure over the eastern equatorial Pacific ocean and high pressure over the western Pacific Ocean, Indonesia, and the Indian Ocean. The Southern Oscillation has been shown to be a reasonable predictor of annual (July-June) precipitation by Hastenrath (1987). The lower-level zonal wind depicts a characteristic relaxation of the climatological trades around the dateline, and anomalous divergence (at least in the zonal component of the flow) over Indonesia. This divergence signifies a shift in the ascending branch of the Walker circulation, and as such it is not surprising that the correlation coefficients between PC1 and precipitation over Indonesia are large and negative.

Why the EDMs perform well over Indonesia: long-term trends. Fig. 15 shows the relationship between the large-scale flow and Indonesian precipitation during MJJA. Plotted are the time series of mean Station based precipitation over all of Indonesia (PR), the Niño3.4 index with polarity reversed (N34; this index is a good measure of ENSO variability, and is defined as SST averaged over 170° W – 120° W, 5° S – 5° N), and the leading two principal components of SLP (predictor set 1) during MJJA (PC1 and PC2). Visual inspection shows a strong relationship between the

time series of mean precipitation and ENSO events (warm ENSO events – El Niño's – are associated with dry conditions during this season), as discussed earlier. Fig. 15 also shows a significant drying trend in precipitation over Indonesia. PC1 and PC2 are closely related to the long term trend in SLP and variations in ENSO, both of which contribute to precipitation variations. The mean correlation between the trend and station precipitation over Indonesia is $r \approx 0.3$, while the mean correlation of N34 with station precipitation is $r = 0.4$. Combined, the trend and N34 produce a mean correlation of $r \approx 0.51$ (note that the trend is nearly uncorrelated with N34; $r \approx 0.1$), and the combined PC1 and PC2 produce a mean correlation of $r \approx 0.56$. This highlights that both the long-term trend and the interannual variability of ENSO are important for linking the large-scale circulation with regional precipitation variations. Similar arguments can be made for other predictor sets.

Employing the EDMs for downscaling and debiasing output from the climate models (GCMs). An underlying motivation for the present study was to develop techniques to downscale and debias estimates of precipitation from the global climate models in the World Climate Research Programme's Coupled Model Intercomparison Project phase 3 (CMIP3) multi-model dataset (Meehl *et al.* 2007). Naylor *et al.* (2007) apply the annual-cycle based EDMs derived in this study (trained on the NCEP reanalysis) to GCM output from the CMIP3 archive and find a considerable reduction in bias from the model simulated precipitation. The bias reduction indicates that the large-scale fields are better simulated than precipitation – not surprising given difficulties in parameterizing tropical convection in those models. The results also suggest that this

technique may be generally applicable as a bias-reduction technique in other areas of the tropics where precipitation is closely tied to the large-scale circulation.

It is clear from Sec. 3 that the EDMs are skillful in downscaling and debiasing interannual variations in regional precipitation from large-scale circulation fields. It is not clear, however, that the most skillful EDM in linking the observed large scale fields to the regional precipitation is also the best EDM for mapping the large scale fields output from the GCMs to regional precipitation. For example, the UWND fields that comprise the predictor fields from the observations tend to have fine-scale spatial structure that is difficult to capture in the GCMs. As a result, when fed output from the GCMS, EDMs based on the observed UWND produce larger biases (for interannual variations) in downscaled precipitation than EDMs based on SLP (not shown). In contrast, the UWND-based EDMs do a good job in debiasing the seasonal cycle.

The strong relationship between ENSO and precipitation over Indonesia suggests that for practical purposes, a simple model that relates Indonesian precipitation to the state of ENSO would suffice for producing a regional estimate of year-to-year precipitation variations. We note, however, that the current generation of coupled general circulation models have serious biases in simulating details of ENSO variability, including biases in the structure, amplitude, and periodicity of ENSO events. In some cases, these biases will also translate to biases in the large-scale predictor fields used to train the EDMs in this analysis. Naylor *et al.* (2007) addressed this issue by using the annual cycle based EDMs to debias the seasonal cycle of precipitation from the CMIP3 models. ENSO variability was incorporated into their estimate through simply adding

observed ENSO variations to the reconstructed seasonal cycle. While that approach ignores any possible changes in ENSO variability with climate change, the serious biases in simulations of ENSO variability in those models justify the methodology.

5. Conclusions and Discussion

Statistical techniques are used to downscale features of the large-scale circulation to regional precipitation over Indonesia. Three different techniques are tested (MCA, CCA, and EOF / regression analysis), using five different combinations of large-scale predictors. Results show that there is skill in downscaling large-scale conditions to regional-scale precipitation, though the skill varies with region, season and large-scale predictor. The following major results are found:

- The strongest relationship between the large-scale circulation and regional precipitation is found over Java, Bali, and the Indonesian Archipelago during the monsoon "transition" season (Sep-Dec). There is a weak to modest relationship in this region during the dry season (May-Aug), and during the wet (Jan-Apr) season results are conflicting across two different precipitation data sets. In the wet season, large-scale zonal wind variations show the strongest relationship with regional precipitation over this region.

- In northern provinces (especially northern Sumatra, Kalimantan, and Sulawesi) the strongest relationship between the large-scale circulation and regional pre-

cipitation occurs during the wet season. There is little to no skill in Northern Sumatra during the dry or transition seasons. Skill in southern Sumatra and Kalimantan tends to track skill in Java, Bali, and the Indonesian archipelago.

- The skill of the downscaling method does not depend sensitively on the method tested. This is not overly surprising as EOF, MCA, and CCA methodologies are all similar in their construction and methodologies.

- Downscaling methodologies that are trained on the annual cycle are an effective means of debiasing the seasonal cycle of precipitation on a regional scale in Indonesia. The annual cycle based downscaling models that incorporate SLP as a predictor are also capable of reconstructing interannual precipitation variations over much of Indonesia during the dry and transition seasons.

- Attempts to attribute skill in the downscaling methods identified ENSO and a long-term trend as important predictors for regional precipitation.

- A new, provincial scale, station-based precipitation data set was developed for investigating relationships between precipitation, rice production, and the large-scale circulation over Indonesia (Appendix A).

Results from this study indicate that empirical downscaling techniques are useful for producing downscaled and debiased estimates of precipitation variations, as well as estimates of the annual cycle of precipitation, using features of the large-scale circulation over Indonesia. These EDMs have also been used to downscale and debias precipitation

from large-scale fields output by the current generation of global climate models (in the CMIP3 record; Naylor et al. 2007). Results herein, and in that study, suggest that these techniques may be useful wherever regional precipitation variations are strongly related to the large-scale circulation.

The purpose of this study was to document the skill of empirical downscaling techniques in relating the large-scale circulation to regional precipitation variations over Indonesia. The study emerged as part of a larger project to assess the impacts of ENSO variations and global climate change on rice production in Indonesia. The original intent of the downscaling models in that context was to debias and downscale results from global general circulation models (especially the CMIP3 archive) to a regional scale. This context has shaped many aspects of this study (for example the large simulation biases in the tropical hydrological cycle of those models have led us to ignore large-scale precipitation as a potential predictor of regional-scale precipitation - large scale, satellite-based precipitation products may show more skill). Almost certainly other efforts at downscaling precipitation over Indonesia or other tropical regions will find other techniques and large-scale predictor variables that more closely suit the particular purpose for those downscaling activities. However, we do expect the general results of this study to be broadly applicable and informative for those efforts.

Acknowledgments.

This work was supported by the National Science Foundation under grant number SES-0433679. NCEP Reanalysis data provided by the NOAA/OAR/ESRL PSD, Boulder, Colorado, USA, from their Web site at `http://www.cdc.noaa.gov/`. Gridded precipitation data were obtained from the University of Deleware. Station precipitation data were obtained from the IRI / LDEO Climate Data Library at `http://iridl.ldeo.columbia.edu/`. Thanks to two anonymous reviewers for their helpful comments on the original version of this manuscript.

APPENDIX A

Methodology for Station-based Precipitation

Station data for the second regional precipitation data set is based on available station data from the GHCN and GSOD data, and the NOAA/NCEP Climate Prediction Center reported precipitation (obtained under the name "NOAA NCEP CPC EVE" from the LDEO INGRID; Ropelewski *et al.* (1985)). Over Indonesia, the GHCN inventory has observations from 1864 (Jakarta Observatory) to present; we use data from 1950-1999. The GHCN data inventory contains observations from 484 different stations, though station coverage is not consistent throughout the period considered in our analysis. In particular, GHCN station coverage drops markedly in 1976 (Fig. 2), and is almost completely absent by 1990 (there are only a few stations with any data at all beyond 1990). The GSOD data inventory contains data from 116 stations over Indonesia, and is available from 1979-1996 (temporal coverage is variable); we use the "estimated precipitation" rather than the "total precipitation" reported in the GSOD data, though differences between the two are minor. The GSOD data set also reports the number of days each month in which a precipitation observation was recorded. In general (and for the stations we select) data coverage is good, though there are some time periods with few observations per month, especially in the early 1990s. We do not

attempt to control for the number of observations each month. The CPC data inventory contains observations from 129 stations from Augsut 1982 through the present, and we use data through 1999 (temporal coverage is variable). We use the total precipitation provided by this data set. All data were obtained from the LDEO INGRID.

In order to construct a homogeneous data set for investigating precipitation variations over the period 1950-1999, we combine data from the three precipitation data inventories described above. We used the following methodology to identify common station observations from the three different data inventories. First, we identified stations that had the same five-digit WMO station number. This resulted in a nearly seamless combination of the GSOD and CPC data inventories. In the GHCN inventory it was found that many stations had the same WMO station number and were distinguished by a different three-digit modifier (NCDC 2007). In these cases, we classified two stations (from two different data inventories) as identical when any of the following criteria were met (many stations met all of these criteria): the stations have the same station name (including different spellings), the same location (latitude and longitude within a tenth of a degree), and / or a high correlation between data points that were common to both records. Finally, all station records were visually examined, and a final decision to combine records was made when clear discrepancies between data from different inventories were small (e.g. large changes in the mean, annual cycle, or variance were not obvious). Of the several hundred stations examined, there were on the order of twenty (or so) instances where the designation of identical stations was not clear; in these cases we did not designate the two stations as identical. When multiple stations

were classified as identical, the station data were averaged together (the averaging was applied only to dates with reported data in more than one station inventory; for dates with only one inventory reporting, the available data were taken as is). Stations that were not classified as identical were retained as independent station records.

The combined records from the three inventories resulted in a new data inventory containing 531 stations with reported data. Of these stations, we retain only the 71 stations with more than thirty years with reported data (this data need not be continuous). These station locations are plotted as open circles in Fig. 1b, and a timeline of the number of stations with reported data is shown as dark shading in Fig. 2. The station coverage is relatively sparse outside of Java and Bali, with some provinces retaining no station records at all (see also Table 1).

Finally, a provincial-scale data set is constructed from the 71 retained station records. There are numerous ways to combine data from different stations in the same province, each with its own set of disadvantages. It was found that a simple average of data from different stations yielded a time series with non-stationary characteristics as stations with missing data are introduced or eliminated from the average. Thus, we *(i)* standardized all station time series within a given province by removing the mean and dividing by the standard deviation, *(ii)* averaged the standardized time series together, *(iii)* multiplied the resulting single time series for each province by the average standard deviation of precipitation over all stations in that province, and *(iv)* added the mean precipitation over all original time series in that province to the single provincial time series. This resulted in provincial time series with much more stationary characteristics,

but also occasionally resulted in negative precipitation reported for a province, especially during the dry season. As this study focuses on explaining precipitation *variance* using the large-scale circulation as a predictor, we retain the negative precipitation values.

APPENDIX B

Statistical downscaling methodology

The first technique, EOF analysis with linear regression, involves decomposing the predictor field into a set of spatial patterns (EOFs $\mathbf{p}_i$) and temporal expansion coefficients (PCs $\mathbf{z}_i$). Linear regression of the predictand field onto each principal component yields spatial maps of regression coefficients ($\mathbf{q}_i$) that can be used to reconstruct the predictand. Given a new map $\mathbf{x}$ of the predictor at some time t, a spatial map of the predictand ($\hat{\mathbf{y}}$) can be obtained via:

$$\hat{\mathbf{y}} = \sum_{i=1}^{M} \langle \mathbf{x}, \mathbf{p}_i \rangle \, \mathbf{q}_i \tag{B1}$$

where M is the number of retained EOF modes, and $\langle \mathbf{x}, \mathbf{p}_i \rangle$ is the projection of $\mathbf{x}$ onto the i'th predictor EOF pattern. For the EOF based EDM, each different field in the predictor data set is scaled to have equal variance so that all fields are weighted equally

(i.e., for predictor set 3, SLP and SHUM are scaled so that each field has the same total variance).

MCA is a technique that identifies patterns in two different fields that explain the maximum amount of squared covariance between the two fields. Again, in this technique each field in the predictor data set is scaled to have equal variance so that all fields are weighted equally. MCA is performed by applying singular value decomposition (SVD) to the temporal covariance matrix between the predictor and predictand fields, resulting in a set of paired spatial maps of the predictor ($\mathbf{p}_i$) and predictand ($\mathbf{q}_i$), and an associated singular value (σ_i). Each pair of patterns can be projected onto the original data to generate a predictor ($\mathbf{a}_i$) and predictand ($\mathbf{b}_i$) temporal expansion coefficient with covariance σ_i. Given a new map $\mathbf{x}$ of the predictand at some time t, a spatial map of the predictand ($\hat{\mathbf{y}}$) can be obtained via linear regression:

$$\hat{\mathbf{y}} = \sum_{i=1}^{M} \frac{\sigma_i \langle \mathbf{x}, \mathbf{p}_i \rangle}{var(\mathbf{a}_i(t))} \mathbf{q}_i \tag{B2}$$

where M is the number of retained singular vectors, and $\langle \mathbf{x}, \mathbf{p}_i \rangle$ is the projection of $\mathbf{x}$ onto the i'th predictor singular vector.

The last technique considered here, CCA, is similar to MCA in that it identifies pairs of patterns between two different data sets, but differs from MCA in that it maximizes the squared correlation between the two data sets. As with MCA and EOF techniques, each field in the predictor data set is scaled to have equal variance so that all fields are initially weighted equally. An EOF prefilter is applied to the predictor and predictand fields prior to performing CCA to ensure that the analysis does not produce spuriously

localized maps. In this study, the EOF prefilter is used to retain the fewest PCs that explain at least 80% of the variance of each field (this amounted to between three to six principal components for the precipitation fields). Singular value decomposition is then applied to the correlation matrix between the retained PCs, yielding pairs of canonical correlation patterns (in EOF space) for the predictor and predictand ($\mathbf{p}_i$ and $\mathbf{q_i}$), an associated canonical correlation (C_i), and temporal expansion coefficients ($\mathbf{a}_i$ and $\mathbf{b}_i$). Given a spatial pattern $\mathbf{x}$ from the predictor field, a prediction $\hat{\mathbf{y}}$ is obtained via:

$$\hat{\mathbf{y}} = \sum_{i=1}^{M} \left[\left(\sum_{j=1}^{N_x} \frac{\left\langle \mathbf{x}, \mathbf{e}_j^x \right\rangle}{\sqrt{\lambda_j^x}} \mathbf{p}_i(j) \right) C_i \left(\sum_{k=1}^{N_y} \sqrt{\lambda_k^y} \mathbf{e}_k^y \mathbf{q}_i(k) \right) \right] \tag{B3}$$

where $\mathbf{e}_j^x$ and $\mathbf{e}_k^y$ are unit-length eigenvectors of the predictor and predictand fields (from the EOF prefilter), λ_j^x and λ_k^y are the associated eigenvalues, and N_x and N_y are the number of retained EOFs from the prefilter.

REFERENCES

Aldrian E, Sustanto RD. 2003. Identification of three dominant rainfall regions within Indonesia and their relationship to sea surface temperature. *Int. J. Climatol.* **23**(12): 1435–1452.

Braak C. 1929. *The climate of the netherland indies. volumes i and ii.* No. 8 in: Verhandelingen, Koninklijk Magnetisch en Meteorologisch Observatorium te Batavia.

Bretherton CS, Smith C, Wallace JM. 1992. An intercomparison of methods for finding coupled patterns in climate data. *J. Climate* **5**(6): 541–560.

Buishand T, Shabalova MV, Brandsma T. 2004. On the choice of the temporal aggregation level for statistical downscaling of precipitation. *J. Climate* **17**: 1816–1827.

Chang CP, Harr PA, McBride J, Hsu HH. 2004. Maritime continent monsoon: Annual cycle and boreal winter variability. In: *East Asian Monsoon*, *World Scientific Series on Meteorology of East Asia*, vol. 2, Chang CP (ed), World Scientific Publishing Co., pp. 107–150.

Christensen JH, Hewitson B, Busuioc A, Chen A, Gao X, Held I, Jones R, Kolli RK, Kwon WT, Laprise R, na Rueda VM, mearns L, Menéndez CG, R ais anen J, Rinke A, Sarr A, Whetton P. 2007. Regional climate projections. In: *Climate Change 2007:*

The Physical Science Basis. Contribution of Working Group I to the Fourth Assessment Report of the Intergovernmental Panel on Climate Change, Solomon S, Qin D, Manning M, Chen Z, Marquis M, Averyt KB, Tignor M, Miller HL (eds), Cambridge University Press, United Kingdom and New York, NY, USA, pp. 847–940.

De Datta SK. 1981. *Principles and practices of rice production*. Wiley and Sons.

Falcon WP, Naylor RL, Smith WL, Burke MB, McCullough EB. 2004. Using climate models to improve Indonesian food security. *Bull. Indonesian Econ. Studies* **40**: 357–379.

Hackert EC, Hastenrath S. 1986. Mechanisms of Java rainfall anomalies. *Mon. Wea. Rev.* **114**: 745–757.

Hamada JI, Yamanaka MD, Matsumoto J, Fukao S, Winarso PA, Sribimawati T. 2002. Spatial and temporal variations of the rainy season over Indonesia and their link to ENSO. *J. Meteor. Soc. Japan* **80**(2): 285–310.

Hastenrath S. 1987. Predictability of Java monsoon rainfall anomalies: A case study. *J. Climate Appl. Meteor.* **26**: 133–141.

Haylock M, McBride JL. 2003. Spatial coherence and predictability of Indonesian wet season rainfall. *J. Climate* **14**: 3882–3887.

Hendon H. 2003. Indonesian rainfall variability: Impacts of ENSO and local air-sea interaction. *J. Climate* **16**: 1775–1790.

Hendon H, Liebmann B. 1990. A composite study of onset of the Australian summer monsoon. *J. Atmos. Sci.* **47**: 2227–2240.

Houze RA, Geotis SG, Marks FD, West AK. 1981. Winter monsoon convection in the vicinity of North Borneo. part I: structure and time variation of the clouds and precipitation. *Mon. Wea. Rev.* **109**: 1595–1614.

IRI / LDEO. 2007. NOAA NCEP CPC EVE. Website accessed 25 November, 2008, IRI / LDEO Climate Data Library. `http://iridl.ldeo.columbia.edu/SOURCES/.NOAA/.NCEP/.CPC/.EVE/`.

Kalnay E, coauthors. 1996. The NCEP/NCAR 40-year reanalysis project. *Bull. Amer. Meteor. Soc.* **77**: 437–471.

Legates DR, Willmott CJ. 1990. Mean seasonal and spatial variability in gauge-corrected, global precipitation. *Int. J. Climatol.* **10**: 111–127.

Matsuura K, Willmott CJ. 2007. Terrestrial precipitation: 1900-2006 gridded monthly time series (Version 1.01). Website accessed 25 November, 2008, University of Deleware. `http://climate.geog.udel.edu/~climate/html_pages/Global_ts_2007/README.%global.p_ts_2007.html`.

McBride J, Haylock M, Nicholls N. 2003. Relationships between the Maritime Continent heat source and the El Niño–Southern Oscillation phenomenon. *J. Climate* **16**: 2905–2914.

McBride J, Nicholls N. 1983. Seasonal relationships between Australian rainfall and the Southern Oscillation. *Mon. Wea. Rev.* **111**: 1998–2004.

McBride JL. 1998. Indonesia, Papua New Guinea, and Tropical Australia: the Southern Hemisphere Monsoon. In: *Meteorology of the Southern Hemisphere*, ch. 3A, Meteorological Monograph No. 49, American Meteorological Society, pp. 89–99.

Meehl GA, Covey C, Delworth T, Latif M, McAvaney B, Mitchell JFB, Stouffer RJ, Taylor KE. 2007. The WCRP CMIP3 multi-model dataset: a new era in climate change research. *Bull. Amer. Meteor. Soc.* **88**: 1383–1394.

Naylor R, Battisti DS, Vimont DJ, Falcon WP, Burke MB. 2007. Assessing risks of climate variability and climate change for Indonesian rice agriculture. *Proc. Natl. Acad. Sci. (USA)* **104**(19): 7752–7757.

Naylor RL, Falcon WP, Rochberg D, Wada N. 2001. Using El Niño/Southern Oscillation climate data to predict rice production in Indonesia. *Climatic Change* **50**: 255–265.

NCDC. 2007a. Global Historical Climate Network (GHCN)-monthly version 2. Website accessed 25 November, 2008, NOAA National Climatic Data Center. `http://www.ncdc.noaa.gov/oa/climate/ghcn-monthly/index.php`.

NCDC. 2007b. Global Surface Summary of the Day. Website accessed 25 November, 2008, NOAA National Climatic Data Center. `http://www.ncdc.noaa.gov/cgi-bin/res40.pl?page=gsod.html`.

Neale R, Slingo J. 2003. The Maritime Continent and its role in the global climate: a G6CM study. *J. Climate* **16**: 834–848.

Oldeman LR. 1975. *An agro-climatic map of Java*. No. 17 in: Contributions form the Central Research Institute for Agriculture, Central Research Institute for Agriculture (Indonesia).

Oldeman LR, Las I, Darwis SN. 1979. *An agro-climatic map of Sumatra*. No. 52 in: Contributions form the Central Research Institute for Agriculture, Central Research Institute for Agriculture (Indonesia).

Qian JH. 2008. Why precipitation is mostly concentrated over islands in the Maritime Continent. *J. Atmos. Sci.* **65**: 1428–1441.

Ropelewski CF, Halpert MS. 1987. Global and regional scale precipitation patterns associated with the El Niño/Southern Oscillation. *Mon. Wea. Rev.* **115**: 1606–1626.

Ropelewski CF, Janowiak JE, Halpert MS. 1985. The analysis and display of real time surface climate data. *Mon. Wea. Rev.* **113**: 1101–1106.

Schmidt FH, Ferguson JHA. 1951. *Rainfall types based on wet and dry period ratios for indonesia with western new guinea*. No. 42 in: Verhandelingen, Kementerian Pehubungan Djawatan Meteorologi dan Geofisik. Plus figures.

Tanaka M. 1994. The onset and retreat dates of the Austral summer monsoon over Indonesia, Australia, and New Guinea. *J. Meteor. Soc. Japan* **72**: 255–267.

Walker GT, Bliss EW. 1932. World weather V. *Mem. Roy. Meteor. Soc.* : 53–84.

Widmann MM, Bretherton CS, Salathe EP. 2003. Statistical precipitation downscaling over the Northwestern United States using numerically simulated precipitation as a predictor. *J. Climate* **16**: 799–816.

Wilby RL, Charles SP, Zorita E, Timbal B, Whetton P, Mearns LO. 2004. *Guidelines for use of climate scenarios developed from statistical downscaling methods*. IPCC Task Group on Data and Scenario Support for Impact and Climate analysis (TGICA). `http://ipcc-ddc.cru.uea.ac.uk/guidelines/StatDown_Guide.pdf`.

List of Figures

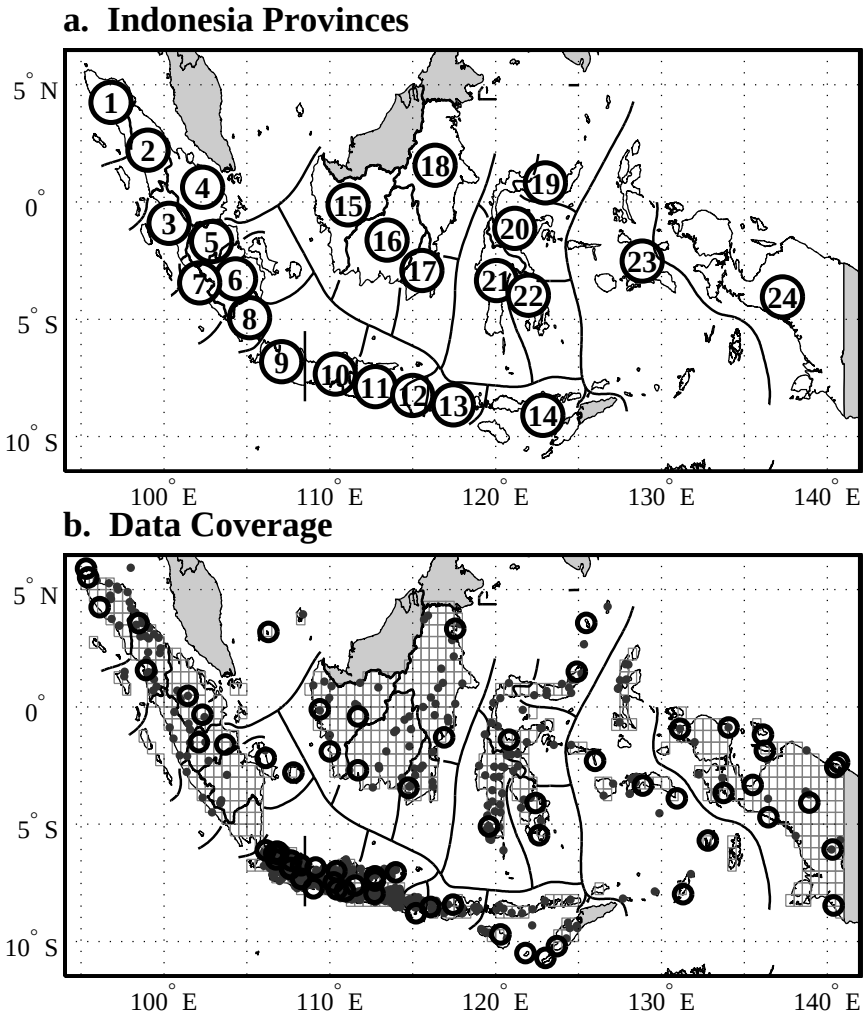

FIG. 1. (a) Provincial scale over which precipitation observations are aggregated. Each number corresponds to the corresponding numbered region in Table 1. (b) Distribution of station precipitation observations. Grey dots indicate all station locations (after combination of the GHCN, GSOD, and EVE inventories) and dark black circles correspond to locations of stations that contribute to the station-based provincial precipitation estimate [these stations have more than 30 yr of reported monthly precipitation (not necessarily contiguous)]. Grid boxes in (b) reflect the 0.5° resolution of the UDel precipitation product.

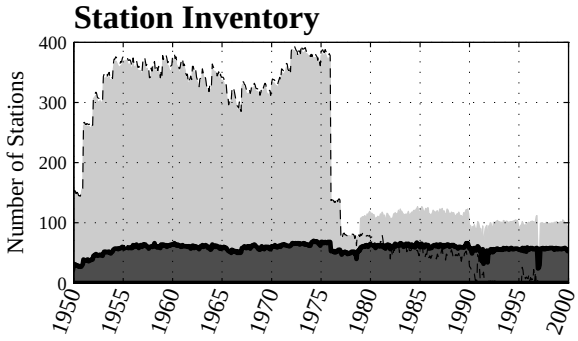

FIG. 2. Number of stations from all three data inventories reporting monthly precipitation from 1950-1999. Light shading indicates the number of stations that reported precipitation for the given month; dark shading (thick black line) indicates the number of stations with >30yr of existing observations, that reported precipitation for a given month; the dashed black line shows the number of stations with reported precipitation for a given month from the GHCN inventory (thus, the difference between the grey shaded curve and the dashed black line indicates the number of stations with reported precipitation from the GSOD and EVE inventories).

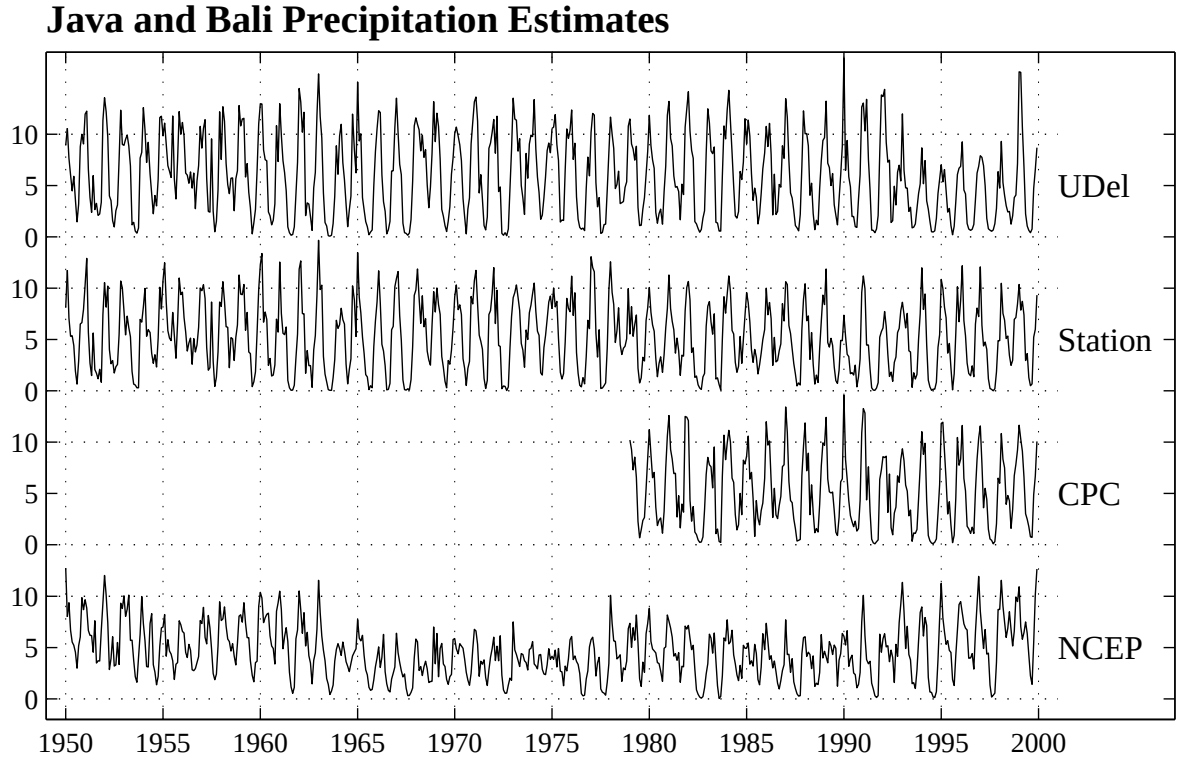

FIG. 3. Four different estimates of precipitation (mm day^{-1}) over the islands of Java and Bali. The first and second curves are obtained as an average over regions 9-12 (Table 1). The third curve is taken from a satellite-based estimate of precipitation from the CPC (IRI / LDEO 2007). The bottom curve is from the NCEP reanalysis. For the bottom two curves, the average is taken over all grid points over the islands of Java and Bali.

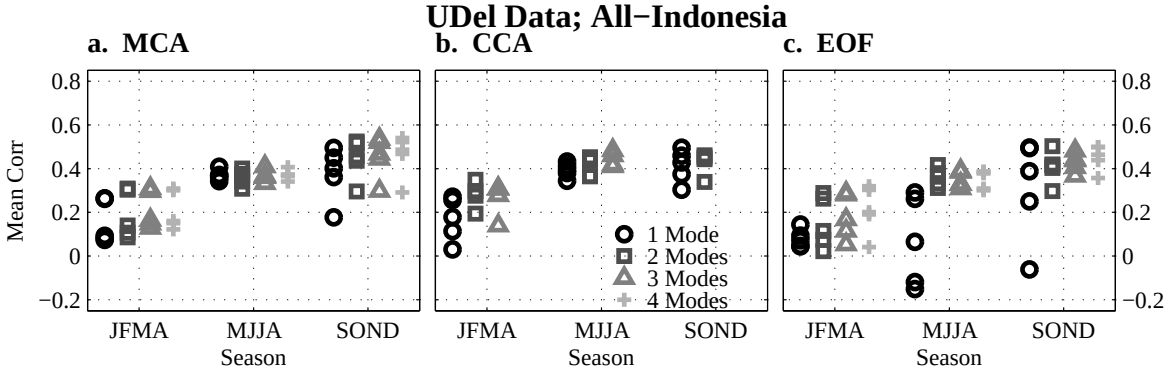

FIG. 4. Mean correlation between predicted (cross-validated) and observed precipitation anomalies (as a function of method, crop season, and number of retained modes) over all of Indonesia, for the UDel data. Correlations are calculated on the provincial scale and then averaged over all provinces to create the all-Indonesia correlation. The three panels depict results for the MCA (left), CCA (middle) and EOF (right) methods. In each panel, results are shown for JFMA, MJJA, and SOND. Black circles, dark grey boxes, grey triangles, and light grey plus-signs refer to reconstructions using 1, 2, 3, and 4 modes, respectively. The correlation is plotted for each of the five EDMs, based on the five different predictor fields (Table 2). For example, the correlation using the MCA technique for SOND using one mode (panel a, SOND, black circles) ranged from about 0.18 to 0.53 for the five different predictor data sets.

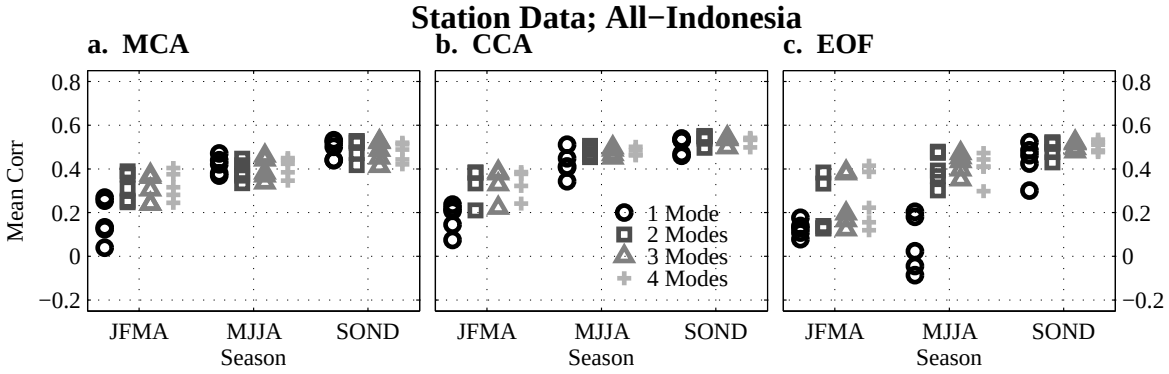

FIG. 5. As in Fig. 4, except for the Station data.

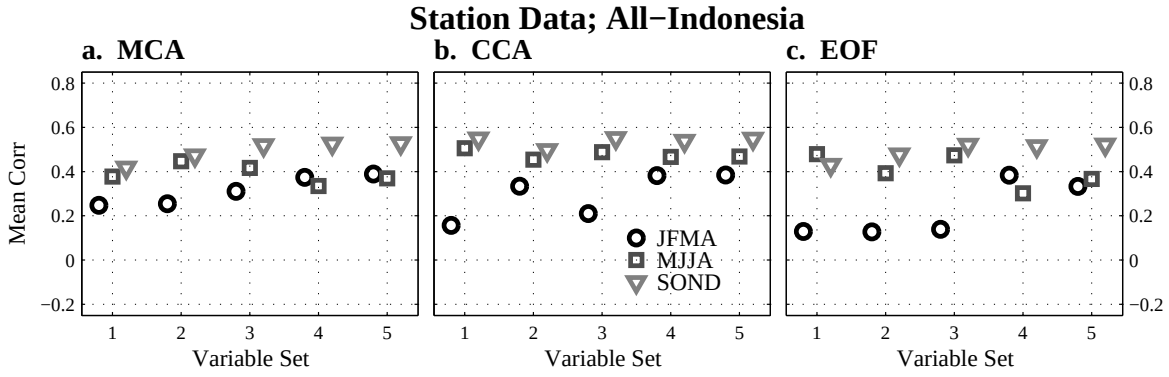

FIG. 6. Mean correlation between predicted (cross-validated) and observed precipitation anomalies (as a function of method, variable, and crop season) for the EDMs calculated using the station data. Correlations are calculated on the provincial scale and then averaged over all provinces to create the all-Indonesia correlation. Precipitation estimates are made using 2 modes, except in cases where the prefilter for CCA retains only one mode. The three panels depict results for the MCA (left), CCA (middle) and EOF (right) methods. For each panel, variable set 1-5 refer to large-scale predictions made with SLP, SHUM, SLP+SHUM, UWND, and UWND+SHUM, respectively. Black circles, dark grey boxes, and grey triangles, depict results for JFMA, MJJA, and SOND, respectively.

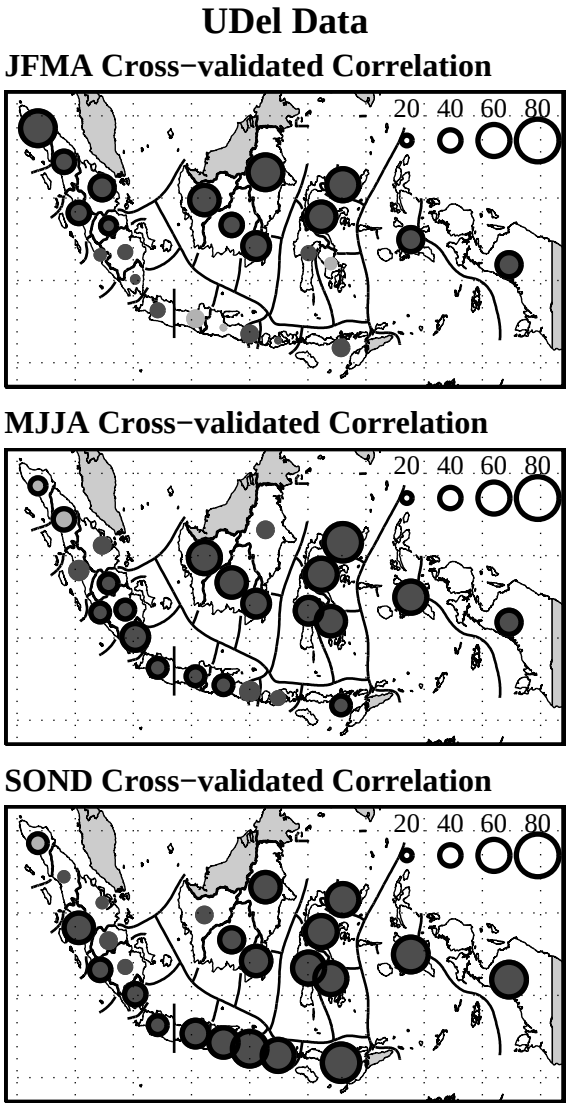

FIG. 7. Correlation (radius of circles; see scale on figure) between the predicted (cross-validated) and actual precipitation anomalies as a function of crop season, for the EDMs constructed from the UDel precipitation data, and using the EOF methodology with predictor set 4 (UWND) and 2 modes. The top, middle, and bottom panels show results for JFMA, MJJA, and SOND. Dark (light) grey circles indicate positive (negative) correlations. Statistically significant correlations are outlined in black.

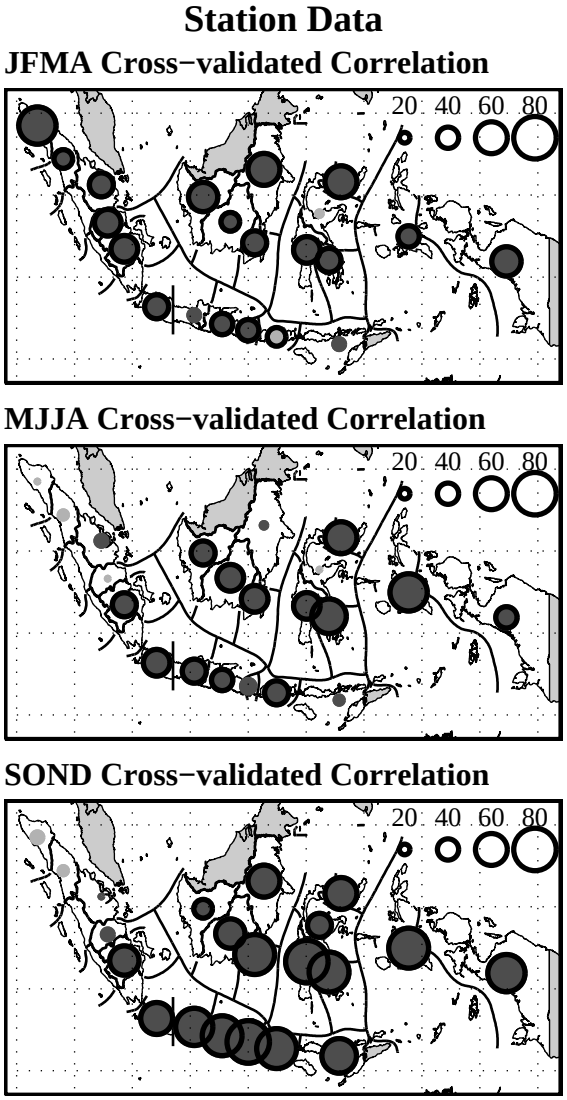

FIG. 8. As in Fig. 7, except for the Station-based precipitation.

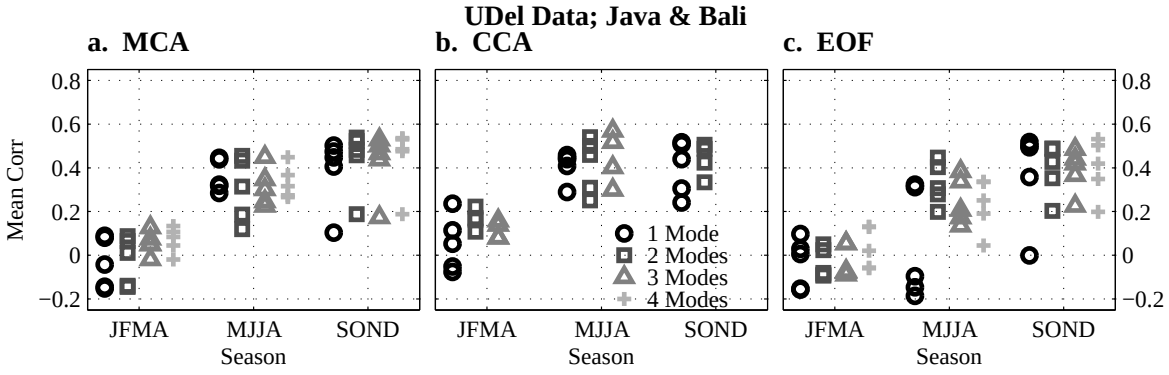

FIG. 9. Mean correlation between predicted (cross-validated) and observed precipitation anomalies (as a function of method, crop season, and number of retained modes) over Java and Bali, for the UDel data. Correlations are calculated on the provincial scale and then averaged over Java and Bali (provinces 9-12 in Fig. 1 and Table 1). The three panels depict results for the MCA (left), CCA (middle) and EOF (right) methods. In each panel, results are shown for JFMA, MJJA, and SOND. Black circles, dark grey boxes, grey triangles, and light grey plus-signs refer to reconstructions using 1, 2, 3, and 4 modes, respectively. As in Fig. 4, correlations are plotted for each of the five EDMs, based on the five different predictor fields (Table 2).

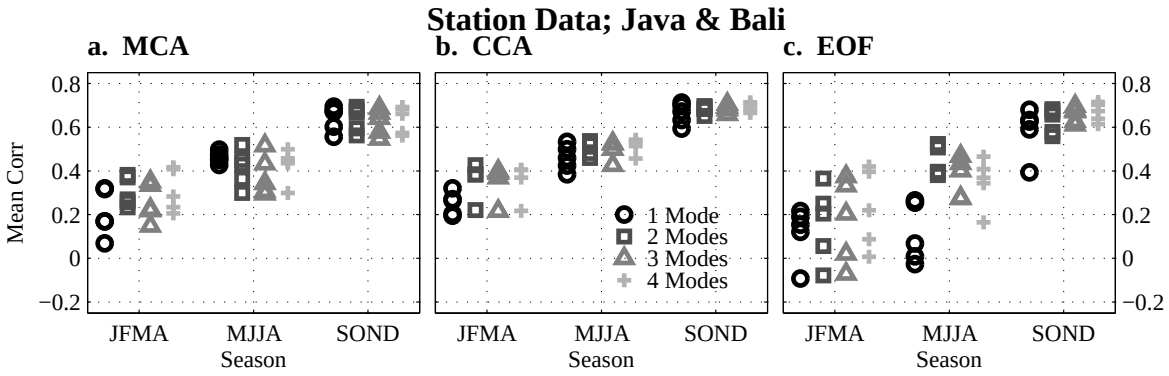

FIG. 10. As in Fig. 9, except for the Station data.

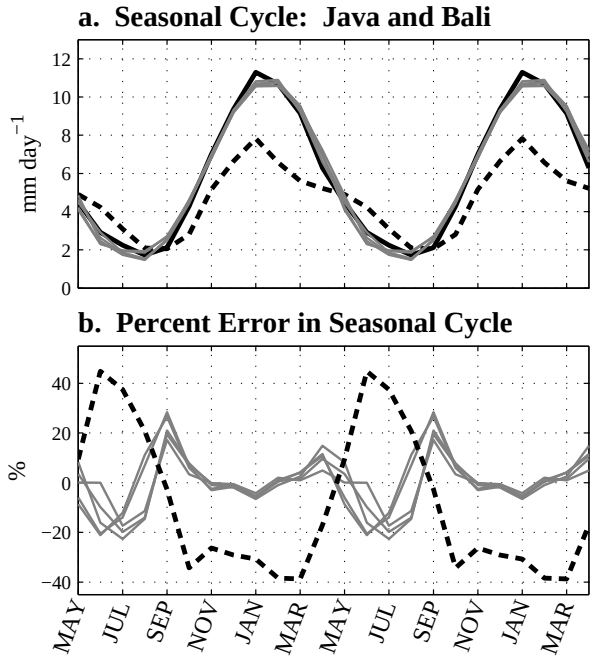

FIG. 11. Reconstructed annual cycle (repeated) of UDel precipitation averaged over Java and Bali (provinces 9-12 from Fig. 1 and Table 1). (a) Annual cycle of precipitation from the UDel based precipitation (thick solid black line), the NCEP reanalysis (thick dashed line), and individually downscaled estimates using EOF methodology applied to the annual cycle from predictor variable sets 1-5 (thin grey lines). (b) Percent difference between UDel based annual cycle of precipitation, and NCEP estimate (thick dashed line) or downscaled estimates (thin grey lines).

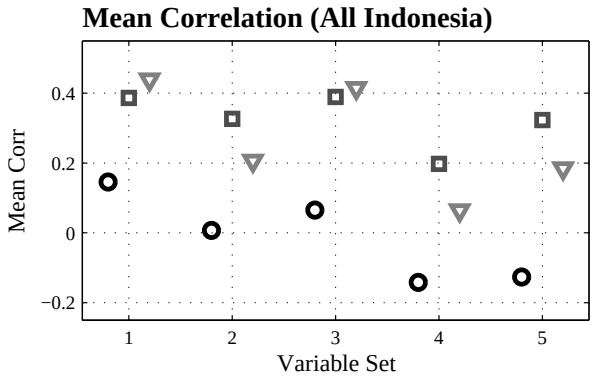

FIG. 12. Mean correlation between predicted and actual precipitation anomalies (as a function of variable and crop season) for the Station data. Correlations are calculated on the provincial scale and then averaged over all provinces to obtain the all-Indonesia correlation. Precipitation estimates are made using the EOF methodology applied to the annual cycle, retaining 3 modes. Variable sets 1-5 refer to large-scale predictions made with SLP, SHUM, SLP+SHUM, UWND, and UWND+SHUM, respectively. Black circles, dark grey boxes, and grey triangles, depict results for JFMA, MJJA, and SOND, respectively.

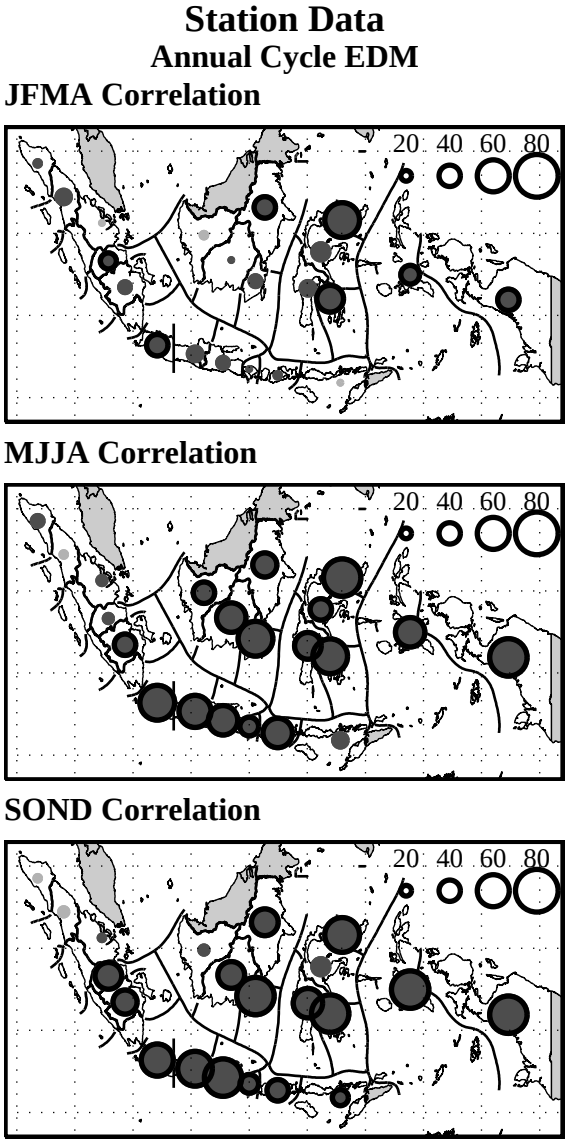

FIG. 13. Correlation (radius of circles; see scale on figure) between the predicted and actual precipitation *anomalies* as a function of crop season, for the Station precipitation data, using the EOF methodology applied to the annual cycle, with predictor set 1 (SLP) and 3 modes. The top, middle, and bottom panels show results for JFMA, MJJA, and SOND. Dark (light) grey circles indicate positive (negative) correlations. Statistically significant correlations are outlined in black.

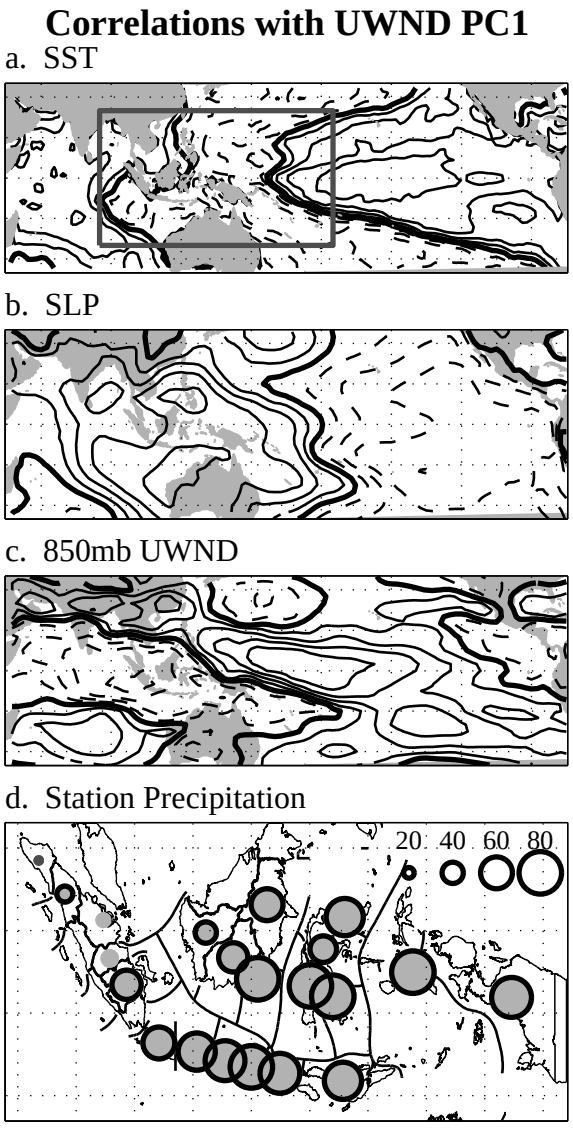

FIG. 14. Contours (contour interval 0.2) of the correlation of UWND PC1 (predictor set 4) for SOND with (a) SST, (b) SLP, (c) 850mb UWND, and (d) regional Station based precipitation. In panels (a)-(c), Solid contours denote positive correlations, dashed contours denote negative correlations, and the zero line is shown as a thick black line. In panel (d) correlations are proportional to the radius of the circle (see scale on figure); dark (light) grey circles indicate positive (negative) correlations (all provinces except Aceh are negatively correlated with PC1), and statistically significant correlations are outlined in black. The UWND PC1 is taken from the full 50 yr of data (not cross-validated).

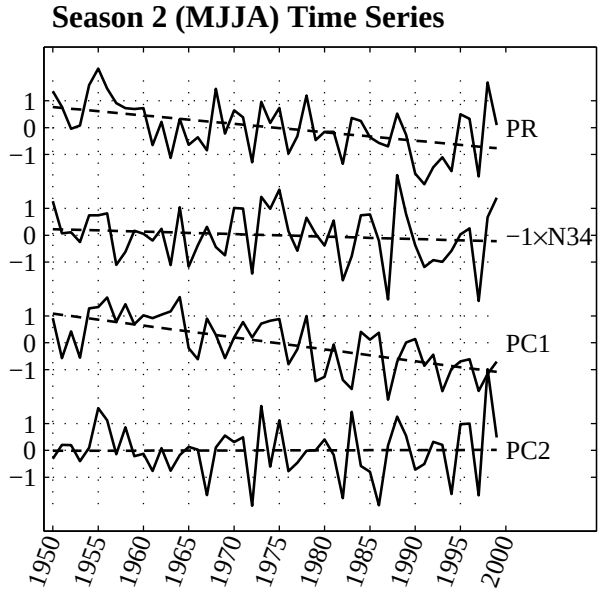

FIG. 15. Standardized time series from MJJA: (PR) mean Station based precipitation over all of Indonesia, (-1×N34) -1 times the Niño3.4 index, (PC1) the leading PC of SLP (predictor set 1) from MJJA, and (PC2) the second PC of SLP (predictor set 1) from MJJA. For each time series, the trend over 1950-1999 is plotted as a dashed line.

List of Tables

TABLE 1. Provinces in Indonesia considered in this analysis, and characteristics of data coverage. "Station" lists the number of stations with >30 yr reported data from the combined station inventories; the total number of stations with any data at all in the combined station inventories is listed in parentheses; the number of months with reported data is listed in brackets. "UDel" lists the number of 0.5×0.5° points in each province, from the UDel data. r(UD, Stat) is the correlation between the UDel and Station-based precipitation estimate (annual cycle has not been removed).

	Province Name	Station: > 30yr (Total) [N mo]	UDel	r(UD, Stat)
1.	Aceh	3 (16) [563]	20	0.63
2.	North Sumatra	2 (25) [597]	23	0.63
3.	West Sumatra	0 (5) [0]	16	–
4.	Riau	3 (9) [585]	32	0.74
5.	Jambi	2 (6) [588]	16	0.69
6.	South Sumatra	2 (7) [600]	32	0.68
7.	Bengkulu	0 (3) [0]	5	–
8.	Lampung	0 (0) [0]	11	–
9.	West Java (incl. Jakarta)	11 (77) [600]	16	0.85
10.	Central Java (incl. Jogyakarta)	6 (75) [591]	12	0.89
11.	East Java	5 (80) [600]	16	0.86
12.	Bali	1 (20) [594]	2	0.77
13.	West Nusa Tenggara	2 (17) [578]	5	0.83
14.	East Nusa Tengara	4 (23) [598]	16	0.85
15.	West Kalimantan	3 (14) [600]	50	0.75
16.	Central Kalimantan	1 (13) [559]	51	0.64
17.	South Kalimantan	1 (11) [565]	15	0.66
18.	East Kalimantan	2 (19) [596]	64	0.56
19.	North Sulawesi	2 (13) [595]	8	0.59
20.	Central Sulawesi	1 (15) [367]	16	0.43
21.	South Sulawesi	1 (29) [584]	21	0.47
22.	Southeast Sulawesi	2 (6) [590]	11	0.68
23.	Maluku	5 (25) [596]	26	0.59
24.	Papua	12 (25) [599]	139	0.55

TABLE 2. Large-scale variable sets used for downscaling precipitation.

	Variable Set	Physical Process
1	Sea Level Pressure (SLP)	Southern Oscillation, Large-scale monsoon
2	850mb Specific Humidity (SHUM)	Hydrological cycle
3	SLP+SHUM	See Variable Sets 1 & 2
4	850mb and 200mb Zonal Wind (UWND)	Large-scale monsoon shear line
5	UWND+SHUM	See Variable Sets 2 & 4

TABLE 3. Projection of the leading (unit length) UWND predictor pattern from each downscaling method (MCA, CCA, EOF) onto the leading and second predictor pattern from each method, as a function of season. Spatial patterns are taken from the full (not cross-validated) 50-yr data.

Season 1 (JFMA)

	MCA1	CCA1	EOF1	MCA2	CCA2	EOF2
MCA1	1	0.97	0.85	0	0.57	0.4
CCA1	0.97	1	0.88	0.03	0.6	0.39
EOF1	0.85	0.88	1	0.49	0.9	0

Season 2 (MJJA)

	MCA1	CCA1	EOF1	MCA2	CCA2	EOF2
MCA1	1	0.99	0.02	0	0.34	0.96
CCA1	0.99	1	0.01	0.01	0.36	0.97
EOF1	0.02	0.01	1	0.82	0.04	0

Season 3 (SOND)

	MCA1	CCA1	EOF1	MCA2	CCA2	EOF2
MCA1	1	0.94	0.87	0	0.22	0.42
CCA1	0.94	1	0.98	0.33	0.1	0.13
EOF1	0.87	0.98	1	0.46	0.25	0